Photoelectrocatalytic activity for water treatment of TiO_2/Ti electrodes prepared by anodization

A. Attyaoui, A. Ben Youssef and L. Bousselmi

ABSTRACT

TiO_2 electrodes are made by anodization of Ti at various applied voltages. The increase of voltage facilitates the generation of anatase and rutile at high potential (superior to 140 V). Photoelectrochemical properties of prepared electrodes are investigated with and without methanol. TiO_2/Ti electrode obtained at 140 V presents high photoelectrochemical properties. The electrode presents better separation of photogenerated electron-hole pairs, high photocurrent and easy charge transfer. The reaction of adsorbed methanol with generated holes increases the photocurrent. When the electrode is anodically biased (application of 1 to 2 V), the photocurrent increases with increased methanol concentration and at alkaline pH.

Key words | anodic oxidation, methanol, photocatalysis, TiO_2, titanium oxide

A. Attyaoui
A. Ben Youssef
L. Bousselmi (corresponding author)
Wastewater Treatment and Recycling Laboratory,
Centre of Water Researches and Technologies,
Technopark Borj Cedria,
BP. 273,
8020 Soliman,
Tunisia
E-mail: *latifa.bousselmi@certe.rnrt.tn*

INTRODUCTION

The photocatalytic process which uses titanium dioxide for the detoxification of chemically polluted wastewater has been the subject of several publications (Bousselmi *et al.* 2004; Zayani *et al.* 2008). However, the main disadvantage of photocatalytic oxidation is the high recombination of photogenerated electrons/holes pairs. In order to limit this recombination effect, researchers have developed an electro-assisted photocatalytic process (Hidaka *et al.* 1999) and photoelectrochemical technology (Jiang *et al.* 2001; Zhang *et al.* 2003; Li *et al.* 2006). In this method, positive potential was applied on the working (TiO_2/Ti) electrodes. Holes were driven to the surface and electrons were swept towards the interior of the semiconductor and driven around the external circuit by the applied potential, possibly inhibiting the recombination of electrons and holes and enhancing the efficiency of photocatalytic oxidation of organic compounds (Christensen *et al.* 2005).

TiO_2 electrodes can be obtained by several methods. In this study, TiO_2/Ti electrodes were prepared using the anodic oxidation method at different potentials. The goal was to identify the most suitable electrode linked to the anodized potential for the electrophotocatalytic process. The crystalline structure and surface morphology of TiO_2 films were examined, as well as the photocatalytic ability of these electrodes in presence of methanol chosen as a model substance for the initial photoelectrochemical characterisation of the electrodes. Methanol belongs to the group of compounds able to react directly with positive holes photogenerated close to the anatase surface (Wahl *et al.* 1995). The electrode with the highest photocatalytic potential was selected for photoelectrocatalytic experiments. The effects of applied anodic potential, methanol concentration and pH on photocurrent were investigated.

doi: 10.2166/ws.2010.712

METHODS

TiO_2/Ti preparation

A titanium disc (99.7% purity) was employed as a substrate for the preparation of the different TiO_2/Ti working electrodes. The material was embedded in a chemically inert resin and, before use, mechanically polishing up to 2500 SiC grade and air-dried at room temperature. The final active area was equal to 1.76 cm^2. The titanium disc was

then immerged in an electrolyte solution, of 0.5 M H_2SO_4; the cathode was a Cu electrode. In this work, anodization voltages (E_{anod}) of 60 V, 80 V, 100 V, 120 V, 140 V and 160 V were used.

Characterization of electrodes

Electrode properties were studied using X-Ray diffraction system (XRD) a Panalytical X'Pert PROMAD X-ray. The surface morphology of films was observed using a Philips series 30 SL scanning electron microscopy (SEM).

Photoelectrochemical procedure

Photoelectrochemical characterization was performed using a potentiostat–galvanostat (Model PGZ 301) and voltamaster 4 software. A 100 ml glass vessel with a quartz window was used as a photoelectrochemical cell with TiO_2/Ti as a working electrode (with an active surface of 1.76 cm^2). A saturated calomel electrode (SCE) was used as reference and platinum wire as counter electrode. All the results are given with respect to the saturated calomel electrode (SCE, +0.241 V/NHE). The electrolyte was an aqueous solution of 0.1 M NaOH (pH = 13), one with methanol and the other without. A 150 W Xenon lamp was employed as an excitation source. The chrono-amperometry curves (I vs. t), voltammograms (I vs. E) and Nyquist diagrams of electrochemical impedance spectroscopy (EIS) investigation were obtained both without and under UV excitation at different pHs (5–13), methanol concentrations (24 to 100 mM) and applied voltages (0–10 V/SCE). The experimental data of the EIS diagrams obtained in the dark and under illumination were analyzed using ZsimpWin3.2 software.

RESULTS AND DISCUSSION

Analytical characterisation of electrodes

The TiO_2 films produced using Ti electrodes are characterized by XRD. For low-voltage anodization (E_{anod} = 60 V and 80 V), there was no diffraction peak of the anatase or rutile phases. However, for TiO_2/Ti electrodes prepared at E_{anod} 100 V, 120 V and 140 V, the anatase phase was detected and the percentage of anatase increased from 0 to 28% with anodization voltage. Furthermore, increasing E_{anod} values to 160 V yielded the formation of a TiO_2 film with a rutile phase (35% Anatase and 14% rutile). Surface morphology and film thickness of the TiO_2/Ti electrodes were characterized by SEM observation. The thicknesses of the electrodes prepared at 100 V, 120 V, 140 V, and 160 V were 14 nm, 18.5 nm, 25 nm and 19.6 nm, respectively. When the voltage is enhanced the current is also increased to produce more heat, which supports the energy to make the TiO_2 film crystallize (Wang *et al.* 2005) on anatase and rutile (Figure 1).

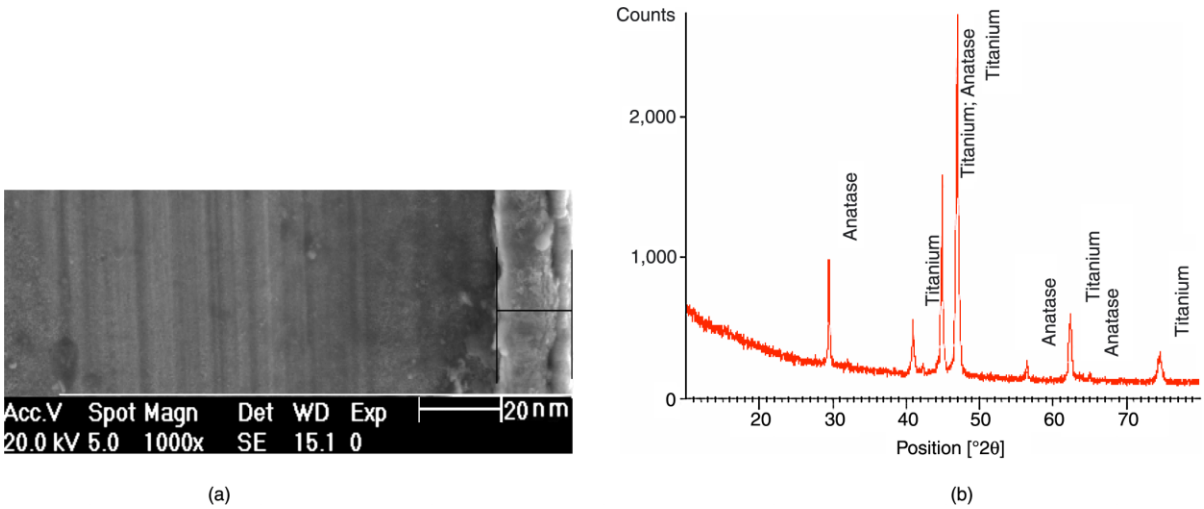

Figure 1 | TiO_2 film (a) SEM observation (E_{anod} 120 V), (b) XRD spectrum (E_{anod} 140 V).

Photoelectrochemical interface behaviour in presence of methanol

Open circuit potential Eoc

The open circuit potential values dropped drastically as soon as the anodized electrodes (TiO_2/Ti) were illuminated with UV light, as a result of the generation of e^-/h^+ pairs in the electrodes. Due to the equilibrium between generation and depletion of photogenerated carriers, the open-circuit potential tended to stabilize under illumination and the unchanging open-circuit potential values meant that steady states of photogeneration were established on the anodized electrode. The open-circuit potential difference (ΔE) between dark and UV illumination was 48 mV. Moreover, the open-circuit potential was independent of anodization voltage between 60 and 160 V (Figure 2). It appears to depend mostly on the nature of the layer formed. Results show that under UV, open-circuit potential values were lower in the methanol solution (24 mM) than in the supporting electrolyte, and that they decreased with the increase of methanol concentration (−0,65 V/SCE, 48 mM). Methanol consumes holes (Pichat 1987) and thus lets more electrons accumulate on the anodized electrode. Multiplying the methanol concentration by two leaded to the same effect on Eoc at this range of concentration.

Cyclic voltammograms (I vs. E)

Cyclic voltammograms for the different electrodes were obtained with a scan rate of 100 mV s^{-1}. Cathodic currents were observed at potentials less than −1.2 V/SCE in both dark and illuminated conditions, evidently due to the electrochemical reduction of H_2O on the anodized electrode. In the dark, anodic curves were similar for all electrodes produced and were characterized by a lower current ($I \approx 0.8\,\mu A/cm^2$) over a wide range of applied potentials characteristic of the passive film. However, under illumination, an anodic peak was observed (Figure 3(a)) and the current of the peak was function of electrode anodization voltage. The TiO_2 film prepared at E_{anod} 140 V produced the highest peak current (Figure 3(b)). This increase in photocurrent was attributed to the oxidation of Ti(III) on Ti(IV) (Oliva *et al.* 2002). Consequently, this peak appeared during illumination, indicating the efficiency of charge separation. The photocurrent peak increased with the increase of methanol concentration (Figure 3(b)). Surface holes decreased as a result of the rapid transfer to methanol and subsequently electrons were trapped in the form of Ti(III) and the oxidation peak of Ti(III) on Ti(IV) increased. Furthermore, the maximum photocurrent peak was registered at E_{anod} 140 V, confirming charge separation efficiency in this electrode.

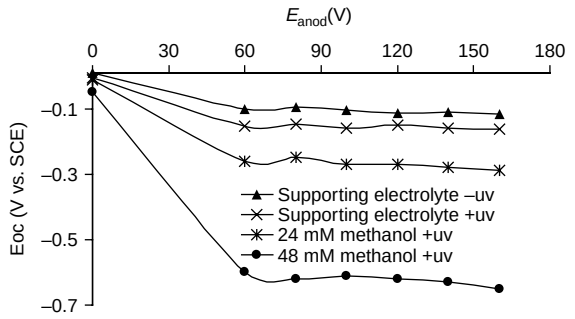

Figure 2 | Open-circuit potential vs. anodization voltage (E_{anod}) in 0.1 M NaOH, in the dark (− UV) and under illumination (+ UV) and in the presence of 24 and 48 mM of methanol.

Photocurrent

The photocurrent was attributed to the following reactions:

$$TiO_2 + h\nu \leftrightarrow (TiO_2 - h) + (TiO_2 - e)(\text{photocurrent})$$

$$OH^- + (TiO_2 - h) \leftrightarrow (TiO_2 - {}^{\circ}OH)$$

The photocurrent density (I) responses of different electrodes in supporting electrolyte under illumination are shown in Figure 4(a). The rise and fall of the photocurrent corresponded well to the illumination being switched on and off. Photocurrent generation occurred in two steps: the first appearing promptly after illumination, and the second, once it reached a steady state.

This pattern of photocurrent was highly reproducible for numerous on–off cycles of illumination (Figure 4(a)). The rapid increase of photocurrents and the steady state observed were both attributed to the photoelectron transport process and interfacial oxidation. Results show that the highest photo response was registered at E_{anod} 140 V (Figure 4(b)), meaning that that electrode was the most photo-sensible. The increase in photocurrent from anodization voltage was due to the percentage of anatase increasing

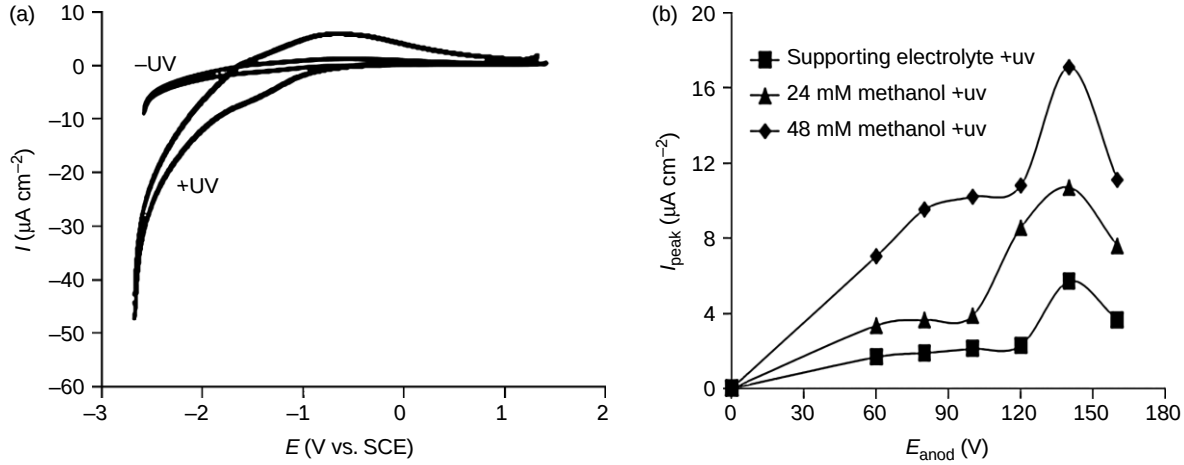

Figure 3 | (a) Cyclic voltammetric curves in supporting electrolyte (0.1 M NaOH) on the electrode anodized at 140 V in the dark and under illumination, at a scan rate of 100 mV/s and (b) I_{peak} vs. Anodization voltage (V) under illumination.

at a higher anodization voltage. However, at E_{anod} 160 V, I decreased due to the heterogeneous structure related to the appearance of the rutile phase. The photocurrent response in the presence of methanol was much higher than the response of the supporting electrolyte. The photocurrent ratio for the two concentrations of methanol was close to 2 for all electrodes, thus corroborating methanol concentration's direct dependence on the photocurrent. The maximum photocurrent response was also registered at 140 V. Methanol belongs to the group of compounds able to react directly with positive holes photogenerated. The photocurrent was generated according to the global reaction: $TiO_2(UV) + CH_3OH + H_2O \rightarrow TiO_2 + CO_2 + 6H^+ + 6e^-$ (Zhang *et al.* 2007). Methanol is oxidized completely in the presence of water to produce CO_2 and protons at the anode or partially to be replaced with either acetic acid or formic acid and formaldehyde in the presence of dioxygen (Gu & Shannon 2007). The formation of intermediates or products is able to act as recombination sites for the electrons. Basing on Wahl *et al.* (1995) work, methanol adsorbed at the anatase phase undergo direct, rapid hole transfer leading to the formation of CH_3O° radical which is an easily oxidized species able to inject an electron to the conducting band of TiO_2. Which excludes formation of the species acting as hole recombination sites like $Ti-O^-/Ti-O^\circ$.

In presence of methanol, at E_{anod} 160 V, I decreased also due to the appearance of the rutile phase. Photoelectrochemical measurements performed with rutile photoanode showed no visible effect of the presence of methanol

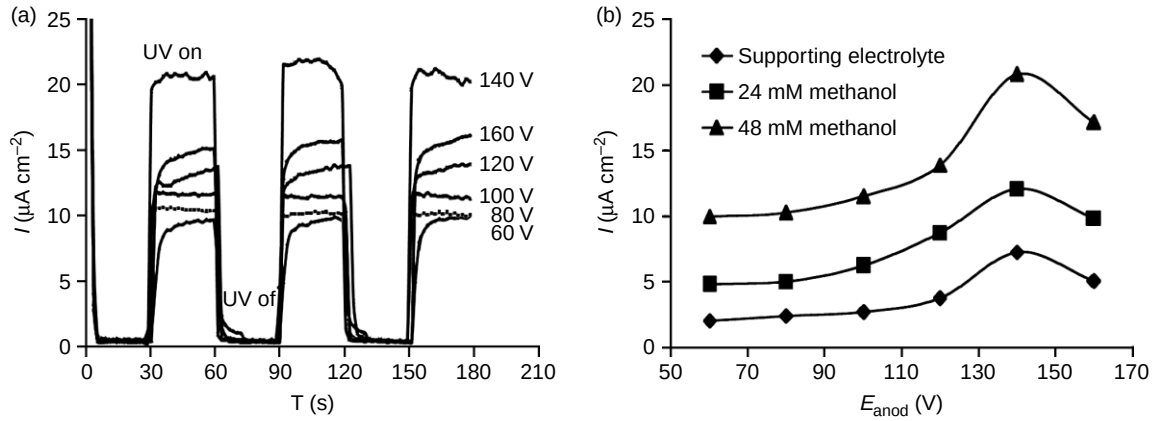

Figure 4 | (a) Photocurrent-time characteristics of different electrodes measured at $E = 1$ V/SCE and (b) photocurrent vs. anodization voltage (E_{anod}).

on the amount of observed photocurrent (Wahl *et al.* 1995). Same study showed similar behaviour of the anatase electrode with photocurrent increasing associated with the photo-oxidation of methanol.

Electrochemical impedance spectroscopy EIS

Electrochemical impedance spectroscopy measurements were carried out covering the $10^5 - 10^{-2}$ Hz frequency intervals with the AC voltage amplitude of 10 mV at the open-circuit potential. Figure 4(a) represents a typical Nyquist diagram for the electrode anodized at 140 V obtained both in the dark and under illumination in the supporting electrolyte.

In the dark, the plots for the Ti/TiO_2 electrodes were very similar except for the electrode obtained at Eimp 160 V. Nyquist diagrams showed a capacitive shape with constant phase element (CPE) behaviour due to the heterogeneity of the electrode surface. Its admittance can be expressed as $Y = Q_0(j\omega)^n$, where n is an exponent of CPE, ω is the angular frequency (rad s^{-1}), and Q_0 is the constant representative for the CPE in F m^{-2} s^{n-1} (Spagnol *et al.* 2009). However, once the UV light irradiation was applied, R//CPE loop behaviour was observed. The diameter of the semicircle formed (Figure 5(a)) corresponding to polarization resistance (*R*p) was found to be greatly influenced by anodization voltage. It further decreased when methanol was added (Figure 5(b)).

The experimental data obtained in the dark and under illumination were well-fitted using the equivalent circuits R_s (CPE) and Rs (CPE//R_P), respectively, where Rs, R_P and (CPE) represent solution resistance, charge transfer resistance for the photoassisted reaction and constant phase elements, respectively. Typical Nyquist diagrams, experimental and fitted, are shown in Figure 5. The capacity *C* value has been extracted based on work done by Brug *et al.* (1984). In the dark, the value of the interface capacity was constant for the different electrodes and corresponds to semi-conductor capacity of TiO_2. Under illumination, it is clear that R_P decreased and the interface capacity (*C*) increased with an increase of anodization voltage (Figure 6). At an anodization voltage greater than 80 V, the interface capacity may correspond to the double layer capacitance (C_{dl}), about 70 μF cm^{-2}. The maximum C_{dl} and the minimum R_P correspond to the 140 V oxidized electrode which means that the charge transfer phenomenon will be easy and fast in this electrode.

Photocatalytic degradation efficiency of this electrode was also highlighted by the work of Wang *et al.* (2007), who demonstrated that the degradation of methyl orange is higher using 140 V oxidised electrode. This result was linked to the increase of the pore quantity, aperture and the content of anatase with the increase of the anodic

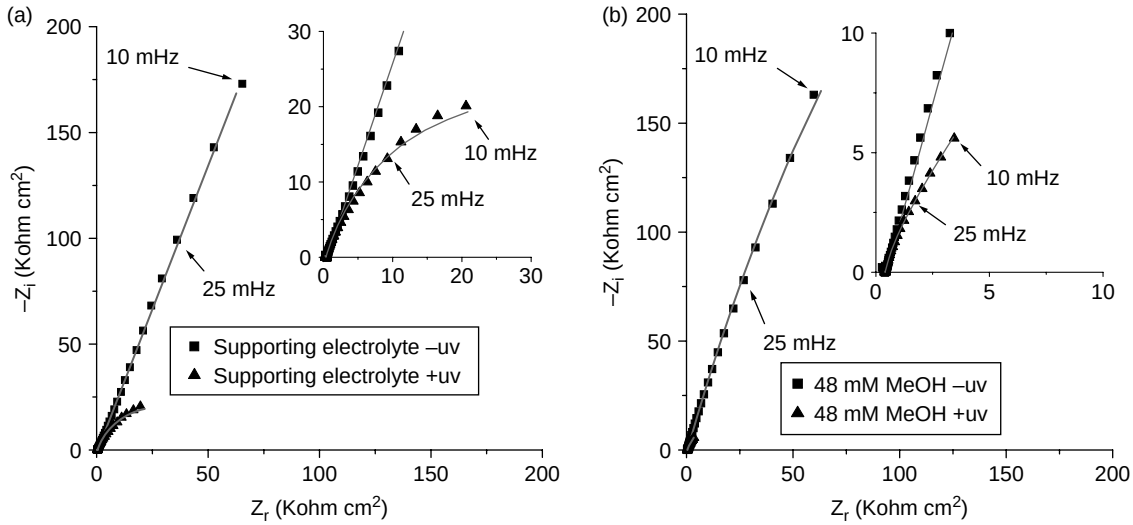

Figure 5 | Nyquist diagrams ($-Z_{im}$ vs. Z_{re}) for the Ti/TiO_2 electrode prepared at 140 V, (a) in 0.1 M NaOH, (b) in the presence of 48 Mm of methanol.

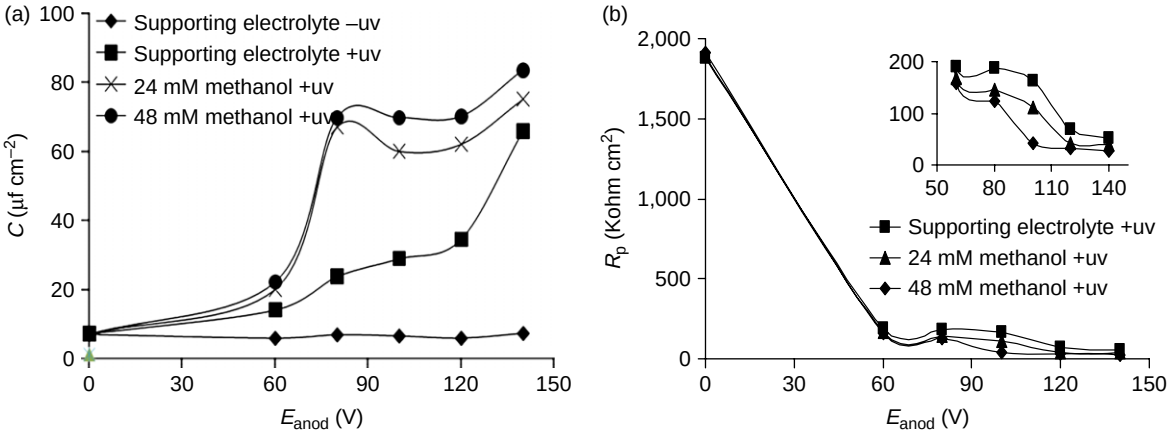

Figure 6 | EIS fitting parameters function of anodization potential, (a) capacity, (b) polarisation resistance (*R*p).

oxidation voltage. TiO_2 films prepared at superior voltage (150 V) had worse degradation effect in comparison with that at 140 V, because of the appearance of rutile in the film.

Based on this photoelectrochemical study, the TiO_2/Ti electrode obtained at anodized potential of 140 V was selected for electrophotocatalytic experiments due to its photosensitivity and charge transfer capacity.

Electrophotocatalysis

Effect of applied potential (photoelectrocatalysis):

The effect of applied potential ($E_{electrocatalyse}$) on photoelectrocatalytic oxidation of methanol was determined both with and without 100 mM of methanol concentration and under and with no UV illumination after 30 min of reaction time at pH 13. Both photocurrent evolution during reaction time and the steady-state value were noted. Figure 7(a) shows the steady state photocurrent obtained after various applied potentials. Under irradiation, the photocurrent increased as the applied potential increased (Figure 7(a)), with a maximum between 1–2 V/SCE as shown in Figure 6(b). In presence of 100 mM of methanol and in the electrolyte support, the maximum was equal to 143.3 and 63.3 $\mu A\,cm^{-2}$, respectively. The increase in photocurrent with positive potential is explained by the fact that the external electric field could reduce the recombination rate of electron-hole pairs.

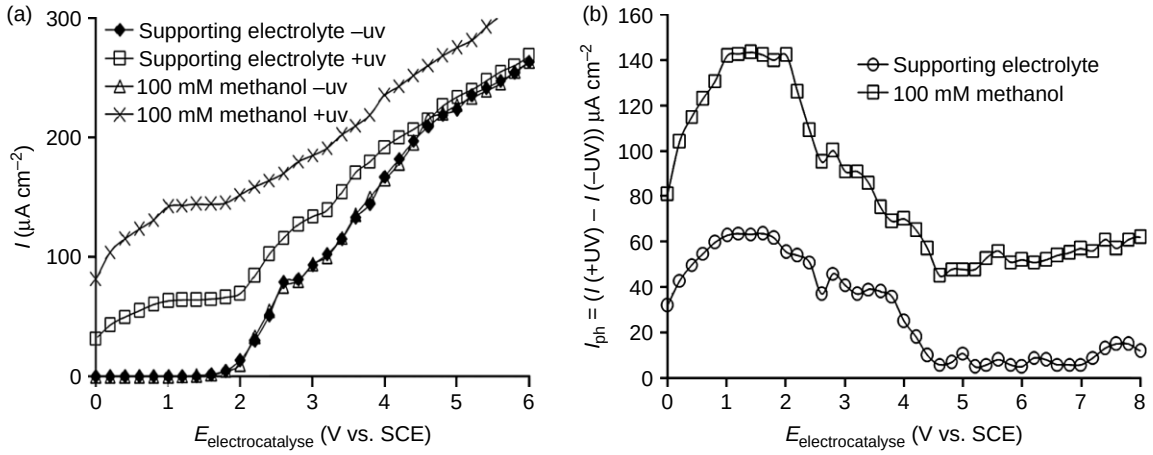

Figure 7 | (a) Current registered vs. electrocatalytic potential (b) calculated photocurrent vs. electrocatalytic potential, electrode anodized at 140 V, degradation time 30 min and pH = 13.

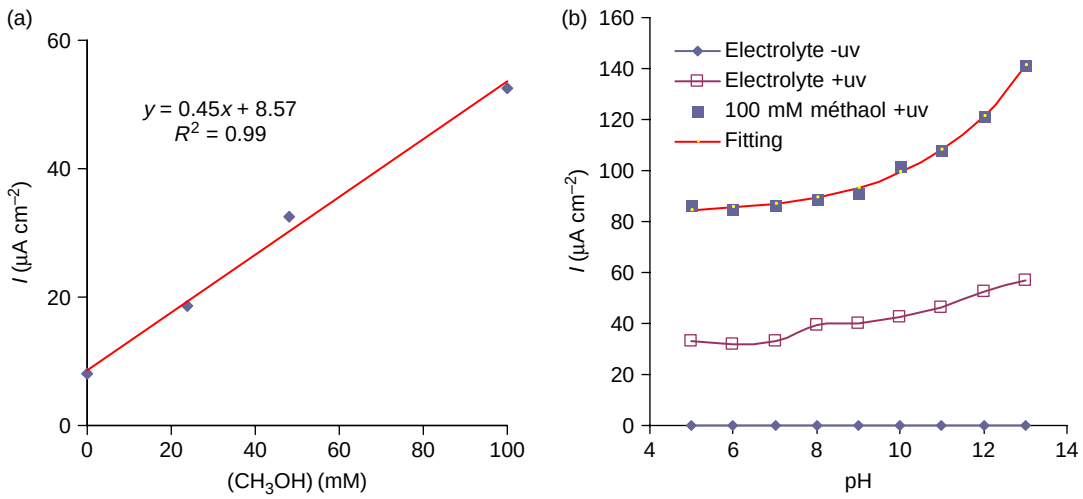

Figure 8 | (a) Photocurrent vs. methanol concentration, pH = 13, (b) photocurrent of the TiO_2 electrode at different pH values both with and without illumination and fitted curve, $E = 1$ V/SCE, 100 mM methanol.

Methanol concentration effect

Photocurrents were determined from I vs. E curves plotted at a scan rate of 100 mV/SCE corresponding to 1 V/ECS. Methanol was added in the electrolyte support (pH = 13). The photocurrent increased with methanol concentration as shown in Figure 8(a). The photocurrent was directly proportional to the concentration of methanol, indicating that the rate of methanol oxidation on the electrode is first order with respect to the concentration of methanol at low concentration. The electrochemical reaction rate constant is equal to $0.45\,\mu A\,cm^{-2}\,mM^{-1}$. This result is in agreement with another work (Zhang *et al.* 2007) but with a lower rate constant. However, it should be noted that the I value obtained at 100 mM of methanol was inferior to that in Figure 7(b). This difference is due to a high potential scan rate, so the steady state is not reached at this methanol concentration.

Effect of pH

The pH value had a significant effect on the adsorption behaviour of the organic compounds on the catalyst surface and on the position of the TiO_2 conduction band (Kavan *et al.* 1993) as well as on OH◦ production. The steady state photocurrent was measured at different pHs between 5 and 13, in both the presence and absence of methanol (100 mM) at applied potential (1V/ECS) (Figure 8(b)). Under irradiation, the same pH effect was obtained both with and without 100 mM of methanol. In the presence of methanol, the photocurrents were greatly increased but showed no obvious variation in the pH range 5–8. This result is mainly due to the direct oxidation of methanol by the photo-generated holes which were presented with a constant concentration in the interface on the acid medium. However, when the pH exceeded 9, photocurrent increased rapidly with pH. One possible reason for this behaviour is that the alkaline pH range favoured the formation of more OH radicals due to the presence of a large quantity of hydroxide ions in the alkaline medium, which significantly enhanced the photocurrent. In this case, the evolution of the photocurrent vs. pH was defined as follows: $I = 0.27\exp(\mathrm{pH}/2.41) + 82.05$ (Figure 8(b)).

CONCLUSION

The study of photocatalytic ability of prepared photoelectrodes was carried out based on the photoelectrochemical behaviour of the interface, which indicated that TiO_2 films prepared with anodic oxidation of Ti at 140 V have the most photocatalytic capacity. Both high photocurrent and easy charge transfer were observed. Photoelectrocatalytic operating conditions were optimized using this electrode and

methanol as model substance. It was found that applying potential from 1 to 2 V/SCE and using an alkaline solution can lead to higher photocurrent. In these conditions, and based on the photocurrent, methanol oxidation on the electrode followed a first order reaction given a low concentration of methanol.

The effect of methanol on photocurrent and charge transfer provides the basis for photoelectrochemical characterisation of anodized TiO_2 electrodes. But photocatalytic activity is strongly linked to the chemistry and physical properties of the pollutant. Thus a comparison of photoelectrocatalytic oxidation of different organic compounds at 140 V oxidised electrode is under development to link photoelectrochemical results with degradation and mineralization of studied compounds.

REFERENCES

Bousselmi, L., Geissen, S. U. & Schroeder, H. 2004 Textile wastewater treatment and reuse by solar catalysis: results from a pilot plant in Tunisia. *Water Sci. Technol.* **49**(4), 331–337.

Brug, G. J., van den Eeden, A. L. G., Sluyters-Rehbach, M. & Sluyters, J. H. 1984 The analysis of electrode impedances complicated by the presence of a constant phase element. *J. Electroanal. Chem.* **176**, 275–295.

Christensen, P. A., Egerton, T. A., Kosa, S. A. M., Tinlin, J. R. & Scott, K. 2005 The photoelectrocatalytic oxidation of aqueous nitrophenol using a novel reactor. *J. Appl. Electrochem.* **35**, 683–692.

Gu, C. & Shannon, C. 2007 Investigation of the photocatalytic activity of TiO_2–polyoxometalate systems for the oxidation of methanol. *J. Mol. Catal. A Chem.* **262**, 185–189.

Hidaka, H., Ajisaka, K., Horikoshi, S., Oyama, T., Zhao, J. C. & Serpone, N. 1999 Photodecomposition of amino acids and photocurrent generation on TiO_2/OTE electrodes prepared by pulse laser deposition. *Catal. Lett.* **60**, 95–98.

Jiang, D., Zhao, H., Jia, Z., Cao, J. & John, R. 2001 Photoelectrochemical behaviour of methanol oxidation at nanoporous TiO_2 film electrodes. *J. Photochem. Photobiol. A Chem.* **144**, 197–204.

Kavan, L., Stoto, T., Gratzel, M. & Fitzmaurice, D. 1993 Quantum size effects in nanocrystalline semiconducting TiO_2 layers prepared by anodic oxidative hydrolysis of $TiCl_3$. *J. Phys. Chem.* **97**, 9493–9498.

Li, J., Li, L., Zheng, L., Xian, Y. & Jin, L. 2006 Photoelectrocatalytic degradation of rhodamine B using Ti/T TiO_2 electrode prepared by laser calcination method. *Electrochim. Acta* **51**, 4942–4949.

Oliva, F. Y., Avalle, L. B., Santos, E. & Cámara, O. R. 2002 Photoelectrochemical characterization of nanocrystalline TiO_2 films on titanium substrates. *J. Photochem. Photobiol. A Chem.* **146**, 175–188.

Pichat, P. 1987 *New J. Chem.* **11**, 135–140.

Spagnol, V., Sutter, E., Debiemme-Chouvy, C., Cachet, H. & Baroux, B. 2009 EIS study of photo-induced modifications of nano-columnar TiO_2 films. *Electrochim. Acta* **54**, 1228–1232.

Wahl, A., Ulmann, M., Carroy, A., Jermann, B., Dolata, M., Kedzierzawski, P., Chatelain, C., Monnier, A. & Augustynski, J. 1995 Photoelectrochemical studies pertaining to the activity of TiO_2 towards photodegradation of organic compounds. *J. Electroanal. Chem.* **396**, 41–51.

Wang, W., Tao, J., Zhang, W., Tao, H. & Wang, L. 2005 Preparation and crystalline phase of a TiO_2 porous film by anodic oxidation. *Rare Metals* **24**, 330.

Wang, W., Tao, J., Wang, T. & Wang, L. 2007 Photocatalytic activity of porous TiO_2 films prepared by anodic oxidation. *Rare Metals* **26**, 136.

Zayani, G., Bousselmi, L., Pichat, P. & Ghrabi, A. 2008 Photocatalytic degradation of the Acid Blue 113 textile azo dye in aqueous suspensions of four commercialized TiO_2 samples. *J. Environ. Sci. Health A* **43**, 202–209.

Zhang, W., An, T., Xiao, X., Fu, J., Sheng, G. & Cui, M. 2003 Photoelectrocatalytic degradation of reactive brilliant orange K-R in a new continuous flow photoelectrocatalytic reactor. *Appl. Catal. A Gen.* **255**, 221–229.

Zhang, Z., Yuan, Y., Fang, Y., Liang, L., Ding, H., Shi, G. & Jin, L. 2007 Photoelectrochemical oxidation behavior of methanol on highly ordered TiO_2 nanotube array electrodes. *J. Electroanal. Chem.* **610**, 179–185.